

Recent Progress in Asymmetric Flow over Slenderbody at High Angle of Attack

Li Zhao¹, Yankui Wang^{2,†}, Zhongyang Qi³

¹Ministry-of-Education Key Laboratory of Fluid Mechanics, Beihang University, Beijing 100191, China

^{2,†}Ministry-of-Education Key Laboratory of Fluid Mechanics, Beihang University, Beijing 100191, China

³Ministry-of-Education Key Laboratory of Fluid Mechanics & Aircraft and Propulsion Laboratory, Ningbo Institute of Technology, Beihang University, Beijing 100191, China

¹zhao2835785464@163.com

^{2,†}wangyankui@buaa.edu.cn

³qizhongyang@buaa.edu.cn

Abstract

At high angles of attack (AoA), the asymmetric flow over a slender body is highly affected by the bluntness and machining tolerance of nose, therefore the investigations of asymmetric flow over slender body have great importance in both academic field and engineering application areas. In present work, the effects of the nose bluntness and manual perturbation are investigated at high AoA ($\alpha = 50^\circ$) to reveal the evolution of the separated flow pattern from open-type on pointed nose to close-type separation on blunted nose and the different periodic characteristics of asymmetric flow changing with the circumferential location of nose-perturbation for the pointed and blunted nose respectively. Wind tunnel experiments are conducted at a subcritical Reynolds number $Re_D = 1.54 \times 10^5$ which is based on incoming free-stream velocity (U_∞) and the diameter (D) of the model in Fig.1. In addition, a micro-particle is fixed to the tip of the nose to highlight the machining tolerance which controls the perturbed asymmetric flow in experimental tests. Moreover, the pressure scanning and surface oil-flow visualization techniques are used to capture the pressure distributions and flow patterns on the model surface.

As a result, there exists two kinds of separated flow patterns, herein open-type and close-type separated flow on the pointed nose and blunted nose surface respectively, which are illustrated in Fig.2 and Fig.3 at $\alpha = 50^\circ$. Secondly, the asymmetric flow over the slender-body can be determined by the artificial perturbation on the tip of nose, both pointed nose and blunted nose model. In the meantime, the asymmetric flow mode over the slender-body can also be determined by the relative circumferential location between the artificial perturbation and separated flow line on the nose surface, i.e., taking the open-type flow separation mode on the pointed-nose model as an example in Fig.4, the flow separation is delayed downstream when the perturbation is located in the windward of the separation line and as a result this side vortex appears lower comparing with the opposite side of the slender-body model which is illustrated in Fig.4(b). Furthermore, the flow separation is promoted upstream when the perturbation is located in the leeward of the separation line and as a result this side vortex appears higher comparing with the opposite side of the slender-body model which is illustrated in Fig.4(c). Therefore, the response of asymmetric flow to the circumferential location of artificial perturbation, i.e. the sectional side force changing with the circumferential location(θ), appears double-periodic for the pointed-nose model which is shown by the B=0 line in Fig. 6. However, with regard to close-type flow separation pattern on the blunted-nose model when B=3 in Fig.5, the artificial perturbation is only in the windward of the flow separation line, and as a result, the response of asymmetric flow to the circumferential location of artificial perturbation can only appear single-periodic for the blunted-nose model, which is shown by B=3 in Fig. 6.

Keywords: slender body, asymmetric flow, bluntness, separation, artificial perturbation

†Corresponding Author: Yankui Wang, Tel: +86 010-82317524, E-mail: wangyankui@buaa.edu.cn

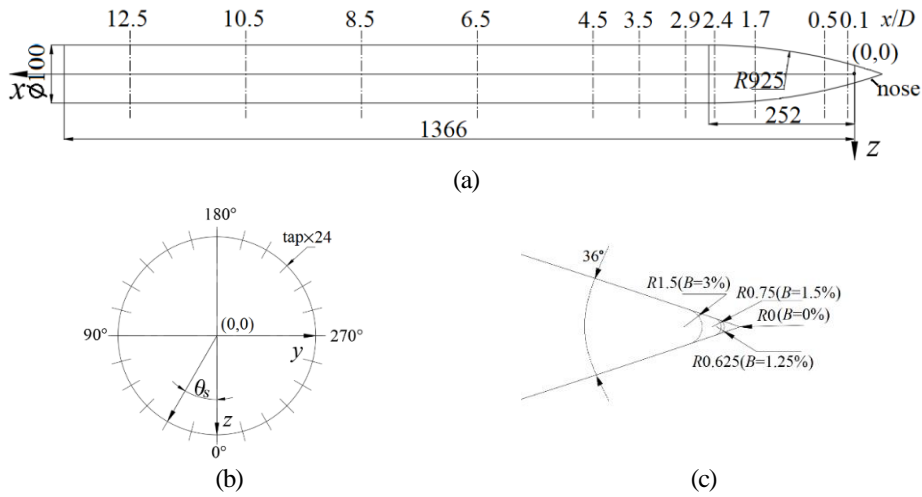


Fig. 1 Schematic diagram showing the test model of a slender body, together with symbol designations. (a) side view; (b) end view. (c) four noses with different bluntness (B). units of length scale are in mm.



Fig. 2 Two patterns of separation over the slender bodies with different nose shapes. (a) open-type separation at a pointed-nosed slender body with $B=0$; (b) close-type separation at a blunt-nosed slender body with $B=3$.

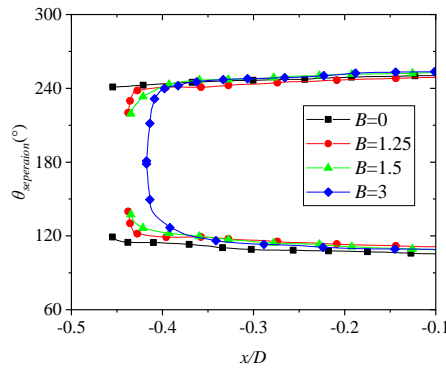
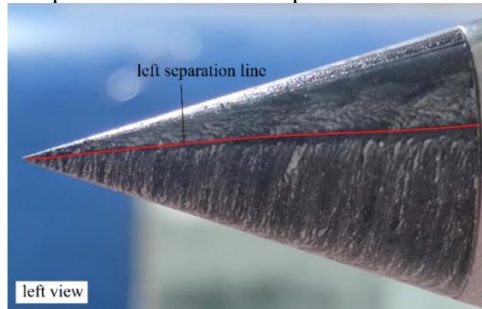
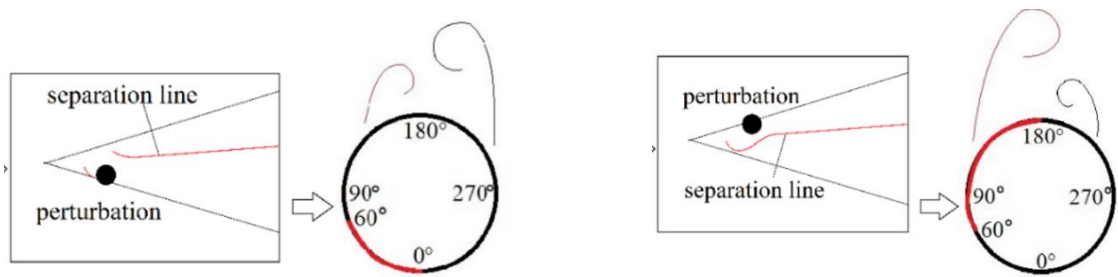


Fig. 3 Variations with x/D of the separation locations at the tip of the nose in the absence of artificial perturbation



(a)oil test result



(b) Perturbation in the windward

(c) Perturbation in the leeward

Fig. 4 The schematic diagram of double-periodic mechanism of perturbed flow over a pointed-nosed slender body with $B = 0$.

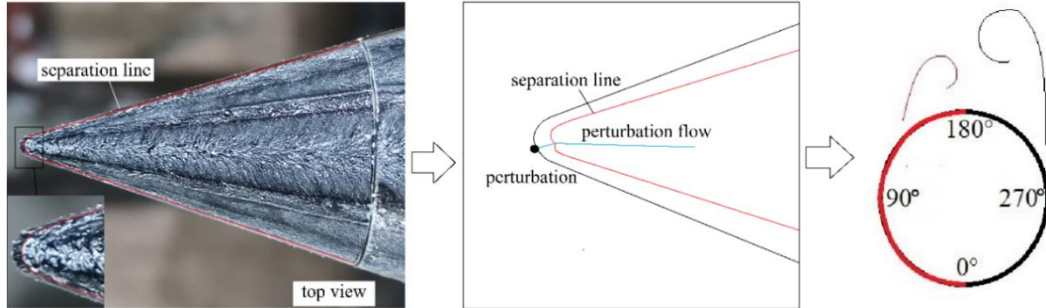


Fig. 5 Schematic diagram of the single-periodic mechanism of the perturbed flow over a blunt-nosed slender body with $B = 3$.

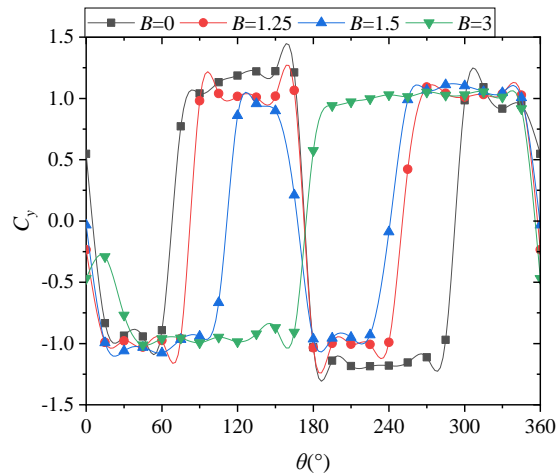


Fig. 6 Variations of C_y with θ in the presence of artificial perturbation at $x/D=3.5$

Acknowledgements

The study is supported by the National Natural Science Foundation of China (11972060&11721202)

References

- [1] D. Xueying, C. Xuerui, W. Yankui, and L. Peiqing, "Influence of nose perturbation on behaviors of asymmetric vortices over slender body," AIAA Atmospheric Flight Mechanics Conference and Exhibit, 2002.
- [2] Q. Zongyang, Z. Siyu, W. Yankui, L. Qian, and W. Jinjun, "Sources of asymmetric flow over the blunt-nose slender body," European Journal of Mechanics - B/Fluids, vol. 75, pp. 372–381, 2019.
- [31] Q. Zongyang, Z. Siyu, W. Yankui, "Bi-stable asymmetry on a pointed-nosed slender body at a high angle of attack," Journal of Applied Physics, vol. 130, no. 2, 2021.